RESIDUAL STRESS IN CRACK STARTER SECTIONS OF DOUBLE TENSION CRACK ARREST SPECIMENS

C. S. Wiesner*, R. H. Leggatt* and B. Hayes*

To assess the crack arrest capability of materials under structurally realistic conditions, the double tension crack arrest test may be used. In this test, a fast running crack is initiated in an embrittled electron beam melt run which is introduced at the edge of the plate. Surface and bulk residual stresses were determined in the melt run and the adjacent region of test material. The maximum residual stresses measured were of the order of the yield strength of the investigated steel. A compressive peak of the transverse membrane residual stress was found at the end of the melt run.

INTRODUCTION

The crack arrest concept provides additional safety for a general fracture avoidance approach, e.g. (1). This concept accepts that crack initiation in local brittle zones or at local stress concentrations is possible. However, the initiated crack will be arrested in the surrounding material, provided its crack arrest toughness is sufficient (2), and a standard test method to determine it has been developed (3). Alternatively, empirical correlation between small scale tests, like the 'Pellini' drop-weight or the drop weight tear test, and structural behaviour can be used to characterise crack arrest properties of a given material (4, 5).

Double Tension Crack Arrest Test

Large scale structurally representative crack arrest tests may be used to simulate the crack arrest behaviour of real structures, e.g. (6, 7). A widely used large scale test is the wide plate double tension test developed in Japan (8). The basic geometry of this test, as it is used by TWI, is shown in Fig.1. A fast running crack is initiated from a sawn notch located in the neck region between the main plate and the secondary loading tab by applying an increasing load to the latter. The sawn notch is located in an embrittled zone which extends into the main plate. The embrittled zone is produced by

* TWI, Abington Hall, Abington, Cambridge, CB1 6AL, UK

remelting a narrow region of the parent material using an electron beam (EB), often referred to as the EB melt run. Since EB welds are not inherently brittle, high carbon silver steel or aluminum wires are added to the melt run to reduce its toughness. The main plate is subjected to the stress level of interest and cooled to the desired test temperature. The outcome of the test is either the arrest of the propagating crack after a short jump (less than approximately two plate thicknesses in length) into the test material, or the complete fracture of the plate. The latter occurs if the driving force for crack propagation, at the moment the crack enters the test material, exceeds the crack arrest toughness of the material. If arrest occurs, the crack arrest toughness can be calculated using the applied stress and the arrested crack length. Strictly speaking, a dynamic analysis is required, however, experimental and numerical results have shown that a static approach gives acceptable results for small arrested crack depth to specimen width ratios, as encountered in double tension tests (9).

Residual Stresses and Crack Arrest

Residual stresses are introduced in double tension specimens by the EB remelting of the embrittled crack starter section. The effect of these residual stresses on crack propagation/arrest behaviour complicates the assessment of the test results. As an example, consider a parent steel containing an EB melt run which extends, say, 100mm into the test plate. After the melt run is introduced, it is expected that the bulk of the melted material and a heated zone around it will be under tensile residual stress transverse and longitudinal to the weld, and the zone of tensile residual stress will extend up to 20 to 30mm beyond the end of the melt run. The resulting distribution will then consist of tensile transverse residual stresses along the melt run, reaching a maximum near the end due to longitudinal shrinkage, and becoming balancing compressive outside the tensile zone, see Fig.2. Assuming that the residual stresses can redistribute elastically in the presence of a fast moving crack in the same way as they would with a slowly growing crack, the resulting contribution to stress intensity is always positive, reaching a peak near the end of the melt run (Fig.2).

Vo (10) carried out numerical analyses regarding the effect of residual stresses around the welded crack starter region in a double tension test specimen on both the static (K^{stat}) and dynamic (K^{dyn}) stress intensity factor. The transverse residual stresses in the weld crack starter were assumed to be tensile in the weld and compressive at the end of it, similar to the assumed distribution shown in Fig.2. The results showed that the influence of residual stresses on the applied dynamic stress intensity factor was dependent on crack speed: lower K^{dyn} were obtained at higher crack speeds. These findings were confirmed experimentally by Smit et al. (11). However, K^{dyn} was always increased by the presence of residual stresses even though they were

compressive in the region ahead of the crack tip. This effect was attributed to the redistribution of the residual stresses during crack propagation; parts of the strain energy released during fracture are transferred to the region ahead of the welded region.

The influence of residual stresses in pre-compressed (in the tensile direction of the specimen) compact crack arrest (CCA) specimens (3) on the obtained crack arrest toughness values has been discussed in reference (12). In a co-operative test programme (13), it was frequently found that the crack arrest toughness values obtained exceeded the applied stress intensity factors at crack initiation. Nevertheless, the crack propagated about 30-60mm into the test material before arrest. It was postulated that this paradox was caused by tensile residual stresses in the weld embrittled and pre-compressed ligament of the specimen. To demonstrate this effect, a specimen was loaded in compression at room temperature and maintained under compression, and then slowly cooled to -170°C (to reduce the fracture initiation toughness). After the temperature had stabilised, the compression load was slowly reduced. Before the compression load was fully released a run/arrest event occurred. This result implies that the pre-compression caused tensile residual stresses ahead of the crack tip which were high enough to initiate and propagate a crack in a specimen at -170°C although the specimens was still under net compressive load. The authors concluded that the crack jump length in a CCA test should be long enough to cross the residual stress field so that the crack arrest toughness can be calculated unambiguously from the applied loading conditions.

The conditions are more complex if the crack arrest properties of weldments are to be investigated. This is so because the welding process itself introduces considerable residual stresses in a welded test plate. A typical residual stress distribution in a welded wide plate is shown in Fig.3 (14). The distribution of transverse membrane residual stresses along the weld line, Fig.3b, is a function of the length of the plate (14). For a weld length of the order of 1m (the typical width of a wide plate double tension specimen) the change from compressive to tensile residual stresses at the edge of the plate occurs rapidly over a distance of approximately 100mm. This means that the end of the embrittled starter section which has a length of typically 100mm is located in a steep gradient of residual stresses, with its tip in either a tensile or a compressive region. The through thickness distribution of transverse residual stresses, Fig.3c, is normally non-linear. The linear component of this distribution, indicated by the hatched line in Fig.3c, represents the bulk residual stress in a welded plate, this being the sum of bending and membrane residual stresses. It can be seen from Fig.3c that the bulk residual stress value at the surface of a plate may be quite different from the 'true' surface residual stress. In a welded double tension test plate, the production of the EB melt run

will substantially alter the welding residual stress state as described in Fig.3. Due to the complexity of the interacting stress fields, predictions are difficult.

The above shows that information on residual stresses due to the EB melt run is necessary to check, if possible, to what extent wide plate double tension crack arrest test results may be affected by residual stresses.

EXPERIMENTAL

Test Specimen

The specimen for residual stress measurement was manufactured using a panel of 25mm C–Mn microalloyed thermo–mechanically controlled process steel (BS4360 Grade 50E mod.) containing 0.06%C, 1.3%Mn, 0.21%Ni and 0.2%Cu. The plate was welded with manual metal arc (MMA) electrodes (AWS E7016–1) containing 0.06%C and 1.3%Mn. The measured yield and tensile strengths of the parent plate were 428 and 520MPa, those of the weld deposit 484 and 580MPa, respectively. The weld preparation was double V, welded in the vertical–up position using strongbacks. The heat input was approximately 2.1kJ/mm. Following welding, a special double tension test plate was prepared with two electron beam crack–starter runs and two secondary loading tabs – one at each end of the MMA weld. This was to enable residual stress measurements to be made in two nominally identical EB melt runs, which was necessary to ensure symmetry during residual stress measurements. The test piece was of dimensions 880mm (along the weld) by 400mm (across it) when the EB crack starter melt runs were deposited. Hence, the stress fields associated with the EB melt runs were remote from each other, and each was representative of that occurring in a standard double tension specimen.

The EB melt run was deposited at a voltage of 140kV and a current of 40mA at a travel speed of 200mm/min. The distance to the workpiece was 350mm. A longitudinal section of a typical EB melt run is shown schematically in Fig.4. The travel of the electron beam (in the opposite direction to crack propagation during crack arrest testing) was started at the same time as the energy of the beam was increased to the operations level. This caused the formation of a fade–in region of approximately 15mm length at the start of the melt run (Fig.4). An immediate full penetration of the remelted crack starter section would have been possible (clear–defined melt run length), however, this would have led to increased porosity in this crucial region of the test specimen.

Residual Stresses Measurements

Surface residual stresses were measured by the centre–hole rosette gauge technique, using a rotating jet of abrasive powder to form the centre–holes. The experimental technique and the formulae for calculating the residual

stresses from the measured strains were as described by Beaney (15). The holes were located in the centre of the weld cap on the face of the test piece from which the EB melt runs were made, which will be referred to as Face 1.

The bulk membrane and bending components of the through-thickness residual stress distribution were determined from strain measurements on small strain gauged blocks of material which were removed from the specimens. The longitudinal (ε_x) and transverse (ε_y) strains runs were combined to give the bulk longitudinal (σ_x) and transverse (σ_y) residual stresses on each face.

$$\sigma_x = -E\,(\varepsilon_x + \upsilon\varepsilon_y) / (1 - \upsilon^2) \quad \text{and} \quad \sigma_y = -E\,(\varepsilon_y - \upsilon_x) / (1 - \upsilon^2) \qquad (1)$$

Elastic properties of E = 207GPa and υ = 0.3 were assumed. The bulk residual stresses on each face of the test piece are, by definition, equal to the sum of the membrane (σ_m) and bending (σ_b) components of the through-thickness distribution of stresses at that location (see Fig.3c), i.e.

$$\sigma_1 = \sigma_m + \sigma_b \quad \text{and} \quad \sigma_2 = \sigma_m - \sigma_b \qquad (2)$$

or conversely:

$$\sigma_m = (\sigma_1 + \sigma_2)/2 \quad \text{and} \quad \sigma_b = (\sigma_1 - \sigma_2)/2 \qquad (3)$$

Index 1 stands for Face 1, index 2 for Face 2.

Results

The transverse surface residual stresses on both ends of the test specimen were entirely compressive in the EB melt run and entirely tensile in the MMA weld metal, peaking at ≈45mm from the fade-in of the EB weld, see Fig.5a. The surface residual stresses along the weld were all tensile in the region investigated, see Fig.5b. On end 1 of the test plate, a minimum in the residual distribution occurred in the MMA weld at 15mm distance from the melt run.

The bulk residual stresses across the weld (Fig.6a) were mainly compressive on Face 1, with a minimum of -500MPa at the tip of the EB weld, and significant but decreasing compressive stresses behind the fade-in of the weld. The stresses across the back of the EB melt run (Face 2) were entirely tensile, but low, see Fig.6a. The bulk residual stresses along the weld (Fig.6b) were mainly tensile but with a compressive peak stress of 250MPa at the fade-in of the EB melt run on Face 1 and with a tensile peak stress of 487MPa on Face 2 in the EB melt run, 30mm behind the fade-in point of the weld.

The membrane and bending residual stresses across the weld are shown in Fig.7a. The membrane stresses are tensile in the EB starter section, exhibit a

compressive peak at the end of the melt run and decrease towards small values with increasing distance from the melt run. The bending stresses across the weld exhibit a tensile peak in the region of the end of the melt run. Their sign does not change in the investigated region. The membrane and bending residual stresses along the weld are shown in Fig.7b. The membrane stresses are primarily tensile with a change into compression at the end of the melt run. They are higher in the EB melt run than in the MMA weld. The bending residual stresses along the weld are relatively small, however a compressive peak of −230MPa was measured at the end of the melt run.

DISCUSSION

Residual Stress Distribution

Residual stresses along a weld are normally tensile in the middle of a welded plate and decrease slightly to become zero at the edge of the plate. The findings in this study (Fig.5b and 6b), basically coincide with this normal behaviour, although the EB melt run was produced after the MMA weld had already introduced a particular pattern of residual stresses. Alterations occur in the residual stress state in the fade−in region of the EB where thermal transients, and the fact that the EB does not fully penetrate the test plate, cause a tensile peak in the longitudinal surface residual stresses. Moreover, a compressive bulk residual stress peak of −250MPa was found at the fade−in. A possible explanation for this will be given below when the transverse residual stress distribution is discussed.

The residual stresses across the weld were more variable. The surface measurements showed compressive stresses in the EB melt run and tensile stresses in the MMA weld (Fig.5a). The bulk stress measurements on Face 1 showed almost the reverse pattern, with tensile stresses at two locations in the EB melt run, and compressive stresses at the fade−in of the EB melt run and at all locations in the MMA weld (Fig.6a). The discrepancy between the bulk and surface stresses indicates the presence of a significant non−linear component in the through−thickness distribution, see Fig.3c.

Before measurements were made, it had been predicted that a compressive peak in the transverse membrane stresses would be found in the MMA weld metal, at perhaps 15 to 45mm from the fade−in of the EB melt run, see Fig.2. As can be seen on Fig.7a, the measured membrane residual stress distribution resembles the central portion of the predicted one and a compressive peak was found, but the peak occurred at the 'fade−in' of the EB melt run. It is postulated that this feature may have been associated with the 'fade−in' of the EB melt run. The shrinkage across the fully−penetrating part of the length of the EB melt run may have been sufficiently greater than that across the fade−in region so that the latter was forced into compression. The Poisson effect of

this compression could have caused the compressive longitudinal stress found at the same location, see Fig.6b.

Figures 5 to 7 show that the fade–in position of the EB melt run is a point where great changes in the residual stress distribution occur. It is assumed that the transients of the fade–in process, i.e. first heating of surrounding regions without remelting, then partly penetrating melt run and finally quasi–steady state melt run production, cause these effects.

Influence on Double Tension Crack Arrest Tests

The influence of longitudinal residual stresses, Fig.5b and 6b, on the crack driving force in a double tension test is not of first order importance. Recent studies, e.g. reference (16), have indicated that a positive stress along the flanks of a crack increase the crack tip triaxiality which promotes crack extension. Whether this effect influences the run/arrest event in a double tension crack arrest experiment remains to be quantified.

The effect of compressive residual stresses across the weld at the fade–in of the EB melt run (Fig.6a, Face 1) and in the adjacent MMA weld could be to retard or arrest the propagation of a crack which might otherwise have continued through this region. However, it should be noted that the bulk residual stresses on the opposite Face 2 of the weld were entirely tensile. Hence, there would be no retardation at the back face, even though the overall membrane stress across the weld is compressive, as Fig.7 indicates. The results by Vo (10) have indicated that the contribution of residual stresses to the crack driving force ahead of the melt run is always positive, even for compressive residual stresses. This implies that compressive residual stresses will not necessarily lead to negative contributions to the applied stress intensity factor which could favour crack arrest in the tests. Nevertheless, if crack fronts in actual double tension tests were found to be arrested at the fade–in of the EB melt run, but to have run ahead of the end of the EB melt run at the opposite face, this would be evidence in support of the possibility that residual stresses may have affected crack arrest behaviour. However, several factors in actual crack arrest tests made a direct comparison impossible:

i. The effect of residual stresses in a double tension test will be reduced by the fact that all actual tests carried out to date were pre–loaded at room temperature to applied stresses of approximately 2/3 yield, which would cause a substantial reduction in the tensile peaks of the residual stress. This was done to simulate the proof tests to which real pressure vessels and storage tanks are exposed before taken into service.

ii. Several parameters affecting the result of a wide plate double tension crack arrest test vary through the thickness of the plate: The end of the melt run is not straight, see Fig.4; the large difference in measured transverse surface and bulk residual stresses (Fig.5a and 6a) indicates that the through

thickness distribution of the actual residual stress is highly non-linear; the central portion of a propagating crack in a wide plate crack arrest test tunnels up to 4 plate thicknesses ahead of the parts which intersect the surface of the plate, i.e., the normal shape of the crack front is also non-linear; and Face 2 of actual test plates is side-grooved which alters the residual stress field and introduces a thickness transient in the region at the end of the melt run.

iii. The limited amount of wide plate double tension specimens which exhibited 'arrest' results makes it difficult to identify with confidence a statistically relevant crack front shape for a given combination of parent material and weld consumable.

SUMMARY AND CONCLUSIONS

Residual stresses were determined in the electron beam melt run crack starter section of wide plate double tension crack arrest specimens. The following conclusions were reached:

i. Longitudinal and transverse residual stresses approaching yield strength magnitude were measured in the crack starter section of the test plate. The transverse membrane residual stresses exhibited a compressive peak at the end of that zone which could retard crack propagation into the test plate.

ii. A direct correlation of the measured residual stresses with arrested crack from shapes in actual double tension crack arrest test specimens was not possible because several features of the residual stress specimen were different from the double tension crack arrest test specimens investigated in other projects.

iii. In non pre-loaded tests, it would be important to quantify the effect of residual stresses on double tension crack arrest test results to determine whether this will influence the outcome of the tests.

iv. Whilst an EB melt run is currently necessary to produce cost effective crack starter section of given lengths in double tension crack arrest test specimens, alternative methods to initiate fast running cracks which do not produce residual stresses should be developed.

Acknowledgement. This work was funded by the Research Members of TWI and the UK Department of Trade and Industry.

REFERENCES

(1) Willoughby AA: 'Crack arrest concepts: Part 1 and 2', TWI Research Bull., Vol.28 (1987), pp.235-240 and 275-277.

(2) Hahn GT and Kanninen MF, Eds.: 'Crack arrest methodology and applications', ASTM STP 711, 1980.

(3) ASTM E1221-88: 'Standard test method for determining plane strain crack arrest fracture toughness K_{Ia} of ferritic steels', ASTM, April 1988.

(4) Smedley GP: 'Prediction and specification of crack arrest properties of steel plate', Int. Journ. Pres. Ves. & Pip, Vol.40 (1989), pp.279–302.
(5) Wiesner CS, Hayes B and Willoughby AA: 'Crack arrest in modern steels and their weldments–comparison between small and large scale tests', Int. Journ. Pres. Ves. & Pip., Vol.56 (1993), pp.369–385.
(6) Willoughby AA and Kawaguchi Y: 'Arrest of long cracks in storage tanks', Proc. Conf. 'Fracture–safe design for large storage tanks', TWI, UK, 1986, Paper 11.
(7) Bristoll P and de Koning AC: 'Crack arrest capability of a controlled rolled, quenched and tempered 3½%Ni steel'. Proc. Conf. 'Fracture–safe design for large storage tanks', TWI, UK, 1986, Paper 12.
(8) Yoshiki M and Kanazawa T: 'On the mechanism of propagation of brittle fracture in mild steel'. Journ. Soc. Nav. Arch. Jap., Vol.102 (1958), p.39.
(9) Wiesner CS, Hayes B, Smith SD and Willoughby AA: 'Investigations into the mechanics of crack arrest in large plates of 1.5%Ni TMCP steel', Fat. Fract. Eng. Mat. & Struct., Vol. 17 (1994), pp 221–233.
(10) Vo T: 'Finite element analysis of dynamic cracking in wide plate specimens'. PhD thesis, University of Wales, Swansea, 1988.
(11) Smit K, Bristoll P and Sypkens Q: 'A study of fracture and arrest when a fast–propagating, brittle crack emanates from a brittle weld into sound 3.5%Ni steel'. Proc. Conf. 'Fracture control of Engineering Structures – ECF 6', pp.243–259, EMAS, 1986.
(12) Hahn GT, Hoagland RG and Rosenfield AR: 'Effects of residual stresses on the weld–embrittled crack arrest test specimen', Written discussion to Ref.(13) in ASTM STP 711, 1980.
(13) Hahn GT, Hoagland RG, Rosenfield AR and Barnes CR: 'A co–operative program for evaluation crack arrest testing methods', ASTM STP 711, 1980, pp.248–269.
(14) Masabuchi K: 'Analysis of welded structures', Pergamon Press, Oxford, 1980.
(15) Beaney EM: 'Accurate measurement of residual stresses on any steel using the centre–hole method', Strain, July 1976, pp.99–106.
(16) Sumpter JDG and Hancock JW: 'Shallow crack toughness of HY80 welds: An analysis based on T stresses' Int. Journ. Pres. Ves. & Pip., Vol.45, (1991), pp.207–222.

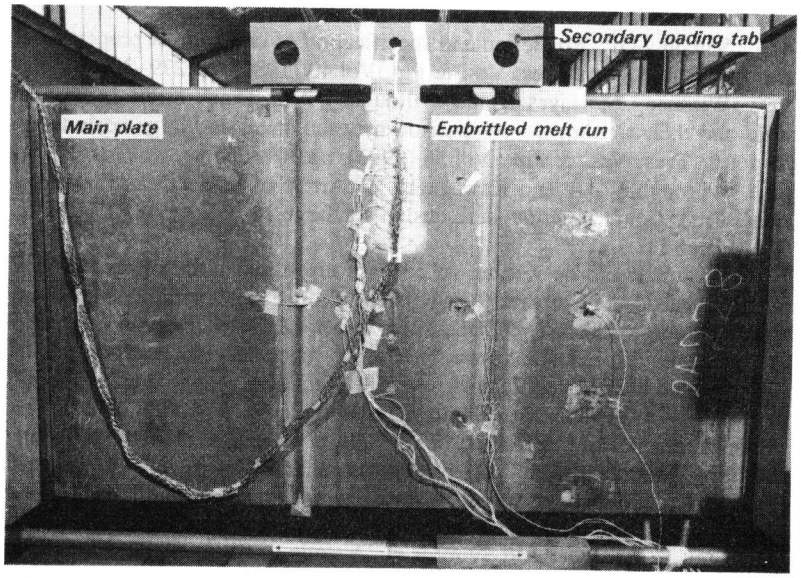

Fig.1 Wide plate double tension crack arrest test set-up.

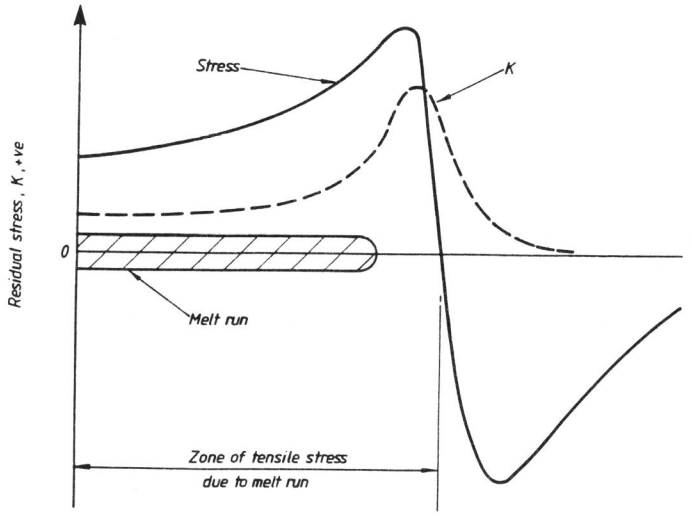

Fig.2 Postulated distribution of residual stress perpendicular to melt run, and variation of static K for crack growing along it.

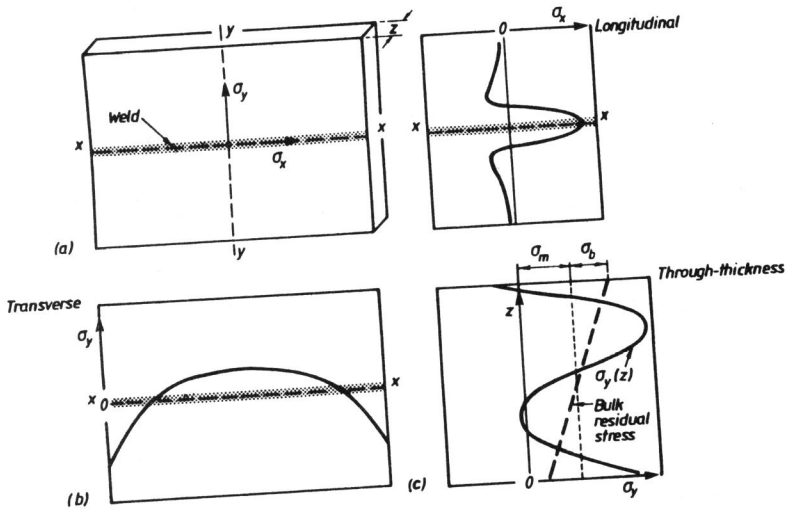

Fig.3 Typical residual stresses in a welded wide plate :[15]

a) *Testplate and longitudinal residual stresses;*
b) *Transverse residual stresses;*
c) *Through-thickness residual stress distribution.*

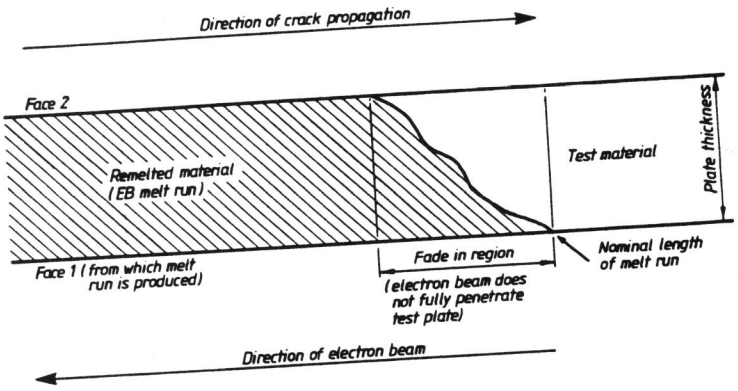

Fig.4 Longitudinal cross-section through wide plate in the 'fade-in' region of the electron beam crack starter section.

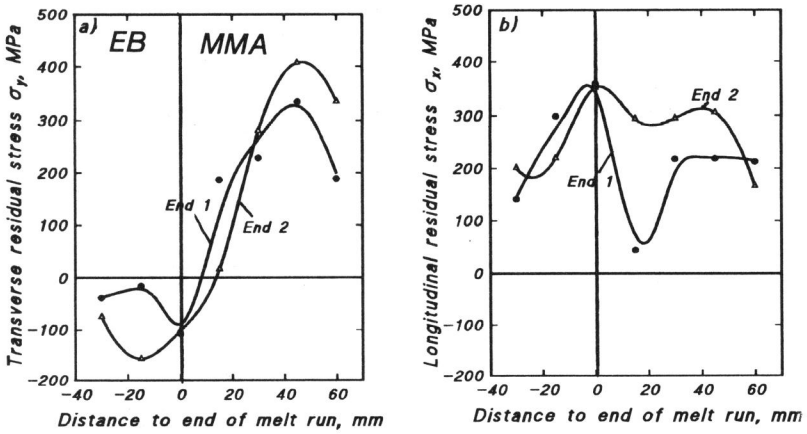

a) *Transverse.*

b) *Longitudinal to the EB and MMA weld centreline.*

Fig.5 Measured surface residual stresses in test specimens (end 1 and 2 refer to the two independent crack starter sections produced).

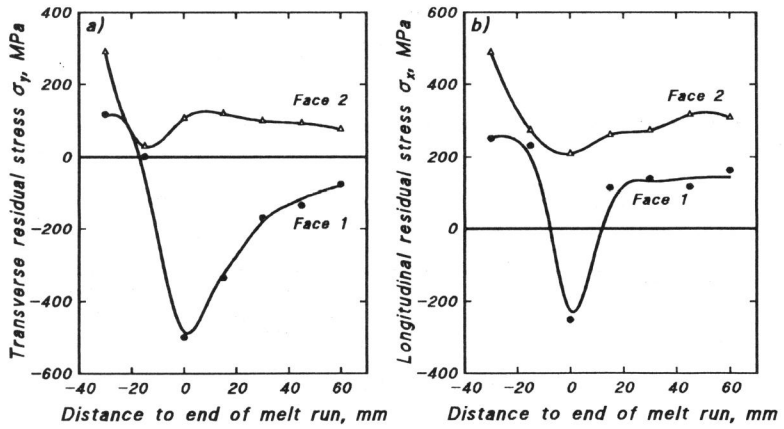

a) *Transverse.*

b) *Longitudinal to the EB and MMA weld centreline.*

Fig.6 Measured bulk residual stresses in test specimens (face 1 is the side from which the EB melt run is deposited):

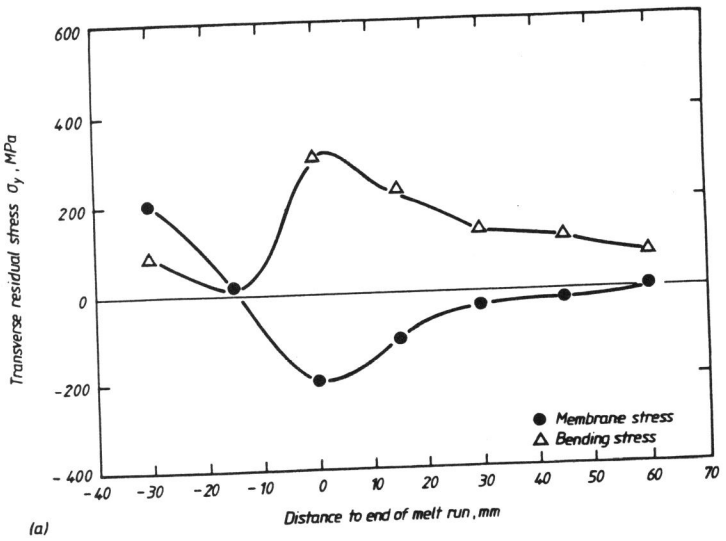

a) *Transverse to the EB and MMA weld centreline;*

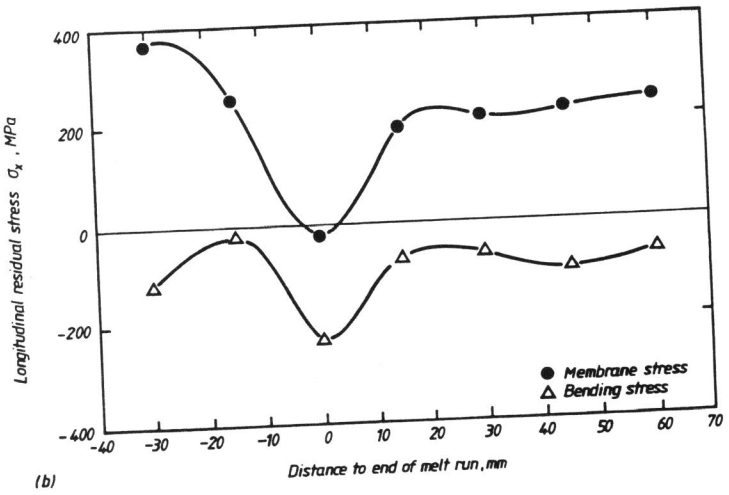

b) *Longitudinal to the EB and MMA weld centreline.*

Fig.7 Measured membrane and bending residual stresses in test specimens: